Left atrial enhancement correlates with myocardial conduction velocity in patients with persistent atrial fibrillation

Brief title: LGE-CMRI correlates with CV in psAF patients

***Rheeda L Ali (PhD)[1]**

Imperial College London, UK

Department of Bioengineering, Imperial College London, SW7 2AZ UK

rheeda.ali@gmail.com

***Norman A Qureshi (PhD, MBBS)**

Imperial College London, UK

National Heart & Lung Institute, Imperial College London, United Kingdom &
ElectroCardioMaths Programme, Imperial College London, London W12 0NN, UK.
n.qureshi@imperial.ac.uk

**Dr. Ali and Dr. Qureshi contributed equally to this manuscript*

Silvia Liverani (PhD)

Queen Mary University of London

School of Mathematical Sciences, Queen Mary University of London, Mile End Road, London E1 4NS,UK

liveranis@gmail.com

Caroline H Roney (PhD)[2]

Imperial College London, UK

Department of Bioengineering, Imperial College London, London SW7 2AZ, UK.
caroline.roney@kcl.ac.uk

Steven Kim (MEng)

Abbot Medical, USA

1 St. Jude Medical Drive. St. Paul, MN 55117
steven.kim@abbot.com

P Boon Lim (PhD, MBBS)

Imperial College London, UK

National Heart & Lung Institute, Imperial College London, United Kingdom &
ElectroCardioMaths Programme, Imperial College London, London W12 0NN, UK.

p.b.lim@imperial.ac.uk

Jennifer H Tweedy (PhD)

Imperial College London, UK

Department of Bioengineering, Imperial College London, SW7 2AZ UK

j.siggers@imperial.ac.uk

Chris D Cantwell (PhD)

Imperial College London, UK

Department of Aeronautics, Imperial College London, SW7 2AZ UK

c.cantwell@imperial.ac.uk

Corresponding author:

Nicholas S Peters (FHRS, PhD, MD)

Imperial College London, UK

National Heart & Lung Institute, Imperial College London, United Kingdom &
ElectroCardioMaths Programme, Imperial Centre for Cardiac Engineering, Imperial College London,
London W12 0NN, UK.

n.peters@ic.ac.uk
011 44 7946 579930

No conflicts.

No relationships with industry.

Sources of Funding

This work was supported by the British Heart Foundation (BHF), grants FS/11/22/28745 & RG/10/11/28457, the ElectroCardioMaths Programme of the Imperial BHF Centre of Research Excellence and NIHR Imperial Biomedical Research Centre.

Total word count: 4500

Abstract

Background: Conduction velocity (CV) heterogeneity and myocardial fibrosis both promote re-entry, but the relationship between fibrosis as determined by left atrial (LA) late-gadolinium enhanced cardiac magnetic resonance imaging (LGE-CMRI) and CV remains uncertain.

Objective: Although average CV has been shown to correlate with regional LGE-CMRI in patients with persistent AF, we test the hypothesis that a localized relationship exists to underpin LGE-CMRI as a minimally invasive tool to map myocardial conduction properties for risk stratification and treatment guidance.

Method: 3D LA electroanatomic maps during LA pacing were acquired from eight patients with persistent AF following electrical cardioversion. Local CVs were computed using triads of concurrently acquired electrograms and were co-registered to allow correlation with LA wall intensities obtained from LGE-CMRI, quantified using normalised intensity (NI) and image intensity ratio (IIR). Association was evaluated using multilevel linear regression.

Results: An association between CV and LGE-CMRI intensity was observed at scales comparable to the size of a mapping electrode:-0.11m/s per unit increase in NI ($P<0.001$) and -0.96m/s per unit increase in IIR ($P<0.001$). The magnitude of this change decreased with larger measurement area. Reproducibility of the association was observed with NI, but not with IIR.

Conclusion: At clinically relevant spatial scales, comparable to area of a mapping catheter electrode, LGE-CMRI correlates with CV. Measurement scale is important in accurately quantifying the association of CV and LGE-CMRI intensity. Importantly, NI, but not IIR, accounts

for changes in the dynamic range of CMRI and enables quantitative reproducibility of the association.

Abbreviations:

CL: Cycle length

CV: Conduction velocity

EAM: Electro anatomical mapping

IIR: Image Intensity Ratio

LGE-CMRI: Late gadolinium enhanced cardiac MRI

NI: Normalized Intensity

Introduction

Success rates of catheter ablation for persistent AF is hindered by our poor understanding of the underlying mechanisms of AF persistence. Central to improving this understanding is the relationship between local myocardial conduction properties and the underlying tissue architecture, determined clinically by estimating myocardial fibrotic burden using late-gadolinium enhanced cardiac magnetic resonance imaging (LGE-CMRI). The challenges to determining this relationship are in part due to limitations and inconsistencies in the acquisition, interpretation and the registration of high-resolution imaging and electroanatomic mapping (EAM) data to allow correlative analyses.

It has previously been established that an electro-architectural relationship exists between myocardial fibrosis and CV on a regional and whole-heart level [1, 2]. However, if such a relationship exists on a localized level, LGE-CMRI may fulfil its potential as a non-invasive tool to map myocardial conduction properties for risk stratification and treatment guidance.

Current 3D EAM systems with high-density multi-electrode contact mapping catheters can provide detailed spatio-temporal information on the functional behaviour of the endocardium. Local CV can give a clear interpretation of underlying tissue health and identify the presence of non-conducting fibrotic tissue through the analysis of wave-front propagation patterns[3, 4]. The accurate evaluation of local CV requires invasive contact mapping with subsequent laborious post-processing of acquired electrograms.

LGE-CMRI is a well-established non-invasive technique to visualise myocardial fibrosis and has been corroborated with histomorphometric validation[5]. Fibrotic atrial imaging has had mixed success due to the current limits of MRI resolution, the patchy nature of atrial fibrosis and difficulties in inter-patient scar-thresholding. As a consequence, several post-processing algorithms and intensity normalisation approaches have been developed to improve the

robustness of LA fibrosis-mapping from LGE-CMRI [6]. Although the extent of enhancement has been associated with conventional markers of atrial structural remodelling such as LA dimension[7], and clinical outcomes following catheter ablation [8], there is continued uncertainty surrounding the exact nature and pathological state of the atrial myocardium delineated by high-intensity regions.

We sought to test the hypothesis that a systematic and objective approach to the acquisition and spatial correlation of CV and LGE-CMRI data can define a reproducible electro-architectural relationship at clinically relevant scales.

Methods

A diagram showing the key steps of the data collection and analysis methodology used in the study is shown in Figure 1

Study Population

Patients with symptomatic persistent AF (based on the classification of AF by published guidelines from the AHA/ACC/HRS/ESC) presenting for their first ablation to Imperial College Healthcare NHS Trust were prospectively enrolled. The study was approved by the Local Research and Ethics Committee for Imperial College Healthcare NHS Trust and written informed consent was obtained from each patient. Patients with contraindications to undergoing LGE-CMRI were excluded from the study.

Data acquisition

Each patient underwent LGE-CMRI prior to the ablation procedure. MRI acquisition was performed using a 1.5T Philips Achieva MR system, and a 5- or 32-element phased-array cardiac coil. LGE-CMRI was performed in the axial orientation 12-20 minutes following the 20ml bolus of gadobenate dimeglumine contrast agent, using an ECG triggered, free-breathing navigator-gated whole heart 3D spoiled gradient echo acquisition sequence. Resolution was at 1.5 x 1.5 x 4mm

and reconstructed to 1.25 x 1.25 x 2 mm. Complete LA coverage was obtained with 40-50 slices. Data were acquired within a window of 100-150ms within each R-R interval depending on heart rates, with a low-high k-space ordering and spectral pre-saturation with inversion recovery (SPIR) for fat suppression. The inversion recovery delay was determined from a Look-Locker sequence, with an inversion time chosen to null myocardial signal. MRI scans were performed in patients in rate-controlled AF. To assess the robustness and reproducibility of the methodology, two patients (denoted throughout as patients G and H) underwent two pre-ablation LGE-CMRI scans, two weeks apart.

Catheter ablation was performed within two weeks from the LGE-CMRI scan. All anti-arrhythmic drugs were discontinued for at least 5 half-lives, and amiodarone was discontinued at least 60 days prior to the ablation procedure. All procedures were performed in the post-absorptive state under general anaesthesia. Transoesophageal echocardiography was performed in all patients once anaesthetised to exclude LA appendage clot, and to subsequently guide transseptal puncture. A deflectable decapolar catheter (Inquiry^{TM}, St Jude Medical, St. Paul, MN, USA) was positioned in the coronary sinus to record electrograms, pace the atrium, and serve as a temporal reference. Single trans-septal punctures were performed using a Brokenbrough needle through a fixed curve long-sheath (SL0, St Jude Medical, MN, USA). Unfractionated heparin was administered to achieve an activated clotting time of 300-350s throughout the procedure.

An impedance-based EAM system (NavX EnsiteTM Velocity, St Jude Medical, MN, USA) was used. The LA geometry and all subsequent data were acquired using a 20-pole (1mm electrodes) double-loop catheter (Inquiry^{TM} AFocusII^{TM}, St Jude Medical, MN, USA) with 4mm electrode spacing. Before each acquisition, the AFocusII catheter was held tangentially to the endocardial surface, enabling stable tissue contact. Patients presenting in AF underwent external DCCV before any mapping was conducted. Following the acquisition of the LA geometry, high-density LA activation mapping was performed. The left atrium was paced from one of more sites (i.e. the

coronary sinus, roof of left atrium and left atrial appendage) at pacing rates of 250ms, 300ms, 350ms and 600ms. The pacing protocol included a drive train of 8 beats to ensure that left atrial capture and activation was consistent (avoiding latency and decrementation), and also to facilitate the stability of AFocusII catheter at the particular site of the left atrium that was being interrogated/mapped.

The LA was paced using a drive train protocol of 8 beats from the coronary sinus, roof and/or left atrial appendage. Unipolar electrograms were recorded and displayed at filter settings of 0.5-100Hz during the procedure, where the 20 recordings together form a kernel as shown in Figure 2A. The electrode positions were projected to the geometry by the EAM system (Figure 2E and 2F). Electrodes more than 5mm away from the surface were disregarded.

Data were acquired at multiple locations on the LA, focused mainly on the posterior endocardial wall where the highest propensity of fibrosis was expected to be found [9]. Local activation times (LATs) were calculated by the EAM system relative to a reference electrode and assigned as the time of the maximum negative gradient of the unipolar electrogram. Electrograms were assessed post-procedurally by an experienced Cardiac Electrophysiologist and those indicative of poor contact or high noise were rejected. Following mapping, pulmonary vein isolation was achieved. All patients were observed for a further 24hrs prior to discharge. No complications were observed in this cohort of patients.

MRI/EAM Segmentation and Registration

The LA epicardial surface on LGE-CMRI images was manually segmented by an experienced Cardiac Radiologist, as shown in Figure 2B, and the epicardial surface was extracted. The EAM surface was co-registered to the MRI surface [10-13]. The accuracy of the registration process was estimated by target registration error [14]. Projected EAM surface electrode positions were mapped

under the computed surface transformation to the MRI surface. The operators performing the ablation procedure were blinded to the generated LA scar-maps derived from the LGE-CMRI.

Local and regional conduction velocity estimation

Conduction velocity was estimated both locally and regionally. Regional CV was estimated by fitting a model of an ideal circular propagating wavefront to the positions and LATs of the 20 electrodes of a given kernel. Additionally, the wavefront radius, r, and residual error, η, of the fit were calculated [15]. High η indicate that the wavefront is not sufficiently smooth within the kernel. Kernels with $\eta < 5$ s/mm were rejected as the wavefront violated the planarity assumptions required by the local CV analysis below.

The local CV is calculated using the principle of triangulation which uses the differences in LATs across unique groups of 3 mapping electrodes (triads) and their interelectrode distance [16]. This approach provides accurate estimates of velocities in areas of just a few mm^2, but assumes planar propagating wavefronts [17]. Triads were only chosen between concurrent recordings within the same kernel to avoid any inter-beat variability of wavefront propagation. The minimum interelectrode distance between any pair of electrodes in a triad was constrained to be greater than the registration error.

Detection and evaluation of left atrial wall intensities from LGE-CMRI

Raw absolute LA wall image intensities were extracted from the LGE-CMRI image as the maximum voxel intensity along a 3mm inward-facing normal from the segmented epicardial surface.

LA wall LGE-CMRI intensities are acquired in arbitrary units and their average brightness and dynamic range varies between images, even between multiple scans of the same subject. Local gadolinium uptake was quantitatively evaluated through two intensity normalisation techniques: 1) Normalised intensity (NI) is calculated from the raw intensity by subtracting the mean intensity

of the LA blood pool and dividing by the standard deviation (SD) of the blood pool voxels [18]; 2) Image Intensity Ratio (IIR) is calculated as the ratio of raw intensity values and the mean intensity of the LA blood pool[19]. Both these metrics convert the raw intensities to quantities which can be compared, and are routinely utilised in LA scar-mapping with LGE-CMRI [1, 8, 19]. The mean and SD of the blood pool were calculated by shrinking the segmented epicardial surface by 5 voxels (3mm). The average NI or IIR value on the area enclosed by each triad of transformed electrode positions was then calculated [20]. A representative map of NI on the segmented surface is shown in Figure 2C.

Reproducibility

A sub-group of two patients had two pre-ablation LGE-CMRI scans, separated by two weeks. Segmentation, registration and construction of the LA scar map were performed independently on each image. A single EAM dataset was used per patient for determining association. The data from each scan were included in the statistical analysis as separate datasets. If the image processing and registration methodology is reproducible, the estimated association should not be significantly different between the two scans of the same patient.

Statistical Analysis

Continuous variables are given as mean±SD; categorical variables are given as percentages. A linear mixed-effects model was used to characterise the relationship between LA wall intensity, using either NI or IIR, and conduction velocity. Likelihood-ratio tests were used to compare if models, fit by maximum likelihood, were significantly different. The inclusion of CL did not significantly improve the model fit and was excluded from the final model.

A multilevel model was used to characterise the relationship between left atrial wall intensity and conduction velocity. Multilevel models provide a mechanism to account for, and quantify, variation

in model intercepts and slopes across patients and cycle lengths. The association between normalised intensity, I, and conduction velocity, V was modelled as

$$V_{ijk} = (\beta_0 + u_j + v_k) + (\beta_1 + \beta_{2j})I_{ijk} + \varepsilon_{ijk}$$

where β_0 is the overall intercept, and $u_j$and v_k are random effects associated with patients and cycle lengths. $\beta_1$captures the effect due to intensity and is the primary parameter of interest in this study, representing the overall association between conduction velocity and intensity across all patients and cycle lengths. The β_{2j} values represent per-patient random slopes; that is, the patient-specific deviation from β_1. Likelihood-ratio tests were used to compare if models, fit by maximum likelihood, were significantly different. The model reported here was statistically significant ($p < 0.001$) compared to all other simpler models without random intercepts or slopes. The inclusion of a random slope for cycle length did not significantly improve the model fit.

Two-sided p-values with $p<0.05$ were considered to indicate statistical significance. Statistical analyses were performed using R version 3.4.3 (The R Foundation for Statistical Computing).

Results

Study Population

Due to the large number of data points collected per patient at multiple paced CL, a total of 8 patients provided sufficient data for the purposes of this study. A summary of the clinical characteristics is given in Table 1. Patients are denoted as A-H.

Data quality

All EAM surfaces were registered to their corresponding MRI surfaces for co-localisation of image intensity with CV. Average target registration errors were 3.08mm (range 1.94-5.71mm).

A total of 267 kernels were acquired across all patients, comprising a total of 5340 mapping points. In total 171 kernels were rejected due to non-planarity of the underlying wavefront ($\eta < 5$ s/mm). A total of 96 complete or partial kernels (mean 12 kernels/patient, range 2-13) remained. An average of 435 triads were formed per kernel (range 1-1140 triads/kernel).

Distribution of conduction velocities and left atrial wall intensities

An overview of the data used in this study is shown in Figure 3 and summary statistics for CV and NI for each patient are given in Table S1. The CV sampled across all patients is given in Figure 3A. The mean CV was 0.85 m/s. A representative example of the distribution of calculated CV is shown in Figure 3B for a kernel from Patient H, paced at a cycle-length of 600ms, with the corresponding regional CV estimate indicated by the red line. Good coherence between the local and regional algorithms was observed across all kernels in the study.

An example of the distribution of gadolinium enhancements using NI (Patient H, second scan) is shown in Figure 3C. The distributions of NI across the entire segmented atrial surface for the first and second scans are shown by the red and blue lines, respectively.

Influence of triad area

Triads were only formed within individual kernels from those electrodes in good contact with the myocardium. Triad areas ranged from 0.12mm^2 to 590mm^2. The change in CV per unit increase in LGE-CMRI intensity, denoted β_1, was measured across all patients and CL. The effect of measurement area on this slope was studied by binning triads by their area and fitting the model to those triads within each bin separately. Bins were chosen as 10mm^2 wide non-overlapping intervals in the range 0-160mm^2. Beyond this range there were insufficient data to generate reliable statistical models. Figure 4 shows the change in the slope with increasing triad area. The magnitude of the slope was found to decrease with increasing area. To address the hypothesis

292 that CV is associated with LGE-CMRI enhancement, specifically at small scales, only those triads
293 with area < 80mm^2 were considered for the remainder of the study.

294 **Association of localised LGE intensity with CV**

295 Conduction velocity correlated with LGE-CMRI intensity (slope = -0.104m/s change in CV per unit
296 increase of NI, $p < 0.001$). The CV at 0 S.D. (model intercept,) was 1.00 m/s, which is within the
297 expected physiological range of healthy myocardium [21, 22]. Per-patient slopes and intercepts are
298 shown in Figure 5A. Six of the per-patient slopes are significantly different from the overall slope
299 (p-values < 0.05). Figure S1 shows corresponding CV and NI at each triad for all kernels from
300 Patient G, scan 2. The overall association and patient-specific association from the statistical
301 model are also highlighted.

302 No random effect relating CL with NI was included in the model (based on the outcome of
303 likelihood-ratio tests). Only one CL (350ms) had an intercept significantly different from the overall
304 intercept. Variations in the intercepts with CL were two orders of magnitude smaller than the
305 overall intercept, suggesting there is negligible change in the relationship with respect to CL.

306 **Reproducibility of LGE-CV evaluation**

307 For Patients G and H, who underwent two LGE-CMRI scans, the images were independently
308 segmented, registered with the clinical data and fused to examine reproducibility. These are
309 shown as G1, G2, H1 and H2 in Figure 5A. For both patients, the slope and intercept for the first
310 and second scans did not differ with statistical significance when using NI.

311 **Comparison of left atrial wall normalisation (NI vs IIR)**

312 LA wall intensity was assessed using NI and IIR. The statistical model was modified to also
313 examine the relationship between IIR with CV. This identified a change in CV of -0.942 m/s per
314 unit increase in IIR ($p<0.001$). The CV was estimated as 1.00m/s at an IIR value of 1.0, which

corresponds to an NI value of 0 S.D. Per-patient slopes and intercepts for the association of CV with IIR are shown in Figure 5B. As for NI, six of the patients have slopes which are significantly different from the overall slope. However, the confidence intervals are larger and reproducibility is poor, as evidenced by a significant difference in the random slopes of H1 and H2.

Discussion

Main Findings

We have demonstrated a localized relationship between local myocardial CV and LA wall LGE in patients with persistent AF on clinically relevant scales comparable to a mapping catheter electrode or ablation lesion. Higher normalised LA intensities represent increased structural fibrotic remodelling and this corresponds to slower CV. The overall estimate for the change in CV with each unit increase in LA intensity was found to be substantially larger in magnitude than previously reported over larger spatial scales. Triad size was found to quantitatively affect the slope, with larger area measurements reducing the magnitude of the corresponding relationship. NI was identified to be a more effective intra- and inter-patient measure of LA intensity normalisation compared to IIR, leading to increased confidence in the estimate of and improved intra-patient reproducibility. There were no significant differences in the relationship across multiple scans of the same patient.

Conduction velocity and LGE-CMRI defined fibrosis

Lower local CV were observed in LA regions with increased fibrotic change as defined by the higher extent of gadolinium enhancement. The conduction delay can be explained by several underlying pathophysiological mechanisms including gap junctional remodelling, Na+ channel abnormalities and heterogeneous cell-coupling between myocytes and fibroblasts [23-25].

Measurement scale

The area subtended by the triads used in the analysis had a clear influence on the resulting beta estimate. In this study, the association is determined using triads of area < 80mm^2, allowing for a more direct translation and relevance to catheter ablation in clinical practice. At the upper end of this range (70-80mm^2), the average maximal edge length of each triad was 15.4mm (range 5.9-20.0mm). For comparison, the typical contact area of the ablation electrode is approximately 10mm^2 (3.5mm diameter). Intuitively, averaging over larger areas diffuses the effect of small-scale variations in the quantities of interest and potentially masks the true localised association between them. In the atrium this is crucial, due to the patchy and non-uniform nature of atrial fibrosis [26]. As shown in Figure 2, gadolinium uptake varies on scales as small as 5mm such as in narrow isthmuses which can promote slow conduction and re-entry [27]. Fukumoto et al evaluated intensities for each of 20 sectors of the atrial wall in each axial slice. The length of each sector is approximately 20mm, which is at the upper end of maximal triad edge length used in the present study and correspondingly the larger values of area in Figure 4. Consequently, at larger areas, localized variations in conduction velocity would be averaged out leading to a reduction in the magnitude of the association between conduction velocity and intensity. This factor may explain the apparent discrepancy between the association (beta estimate) of the present study (β_1: -0.942m/s/IIR), at smaller spatial scales of areas < 80mm^2, and that of Fukumoto et al (β_1: -0.34m/s/IIR). To explain this, Figure 4 also shows the same area dependency plot expressed in terms of IIR where the red and blue dotted lines mark the beta estimates from our study and that of Fukumoto *et al* respectively. The IIR beta estimate of -0.34, found in Fukumoto *et al* for persistent AF patients, is of smaller magnitude than the IIR beta estimate of -0.94 reported here, but is consistent with our findings, if measurement area is taken into consideration. This further emphasizes the importance of resolution when quantitatively comparing quantities.

Reproducibility

While both scans for each patient in the reproducibility sub-study were compared with the same EAM data, our experience suggests that the segmentation and co-registration steps are most prone to the introduction of errors. Importantly, the relationship between CV and NI within each pair of datasets were statistically indistinguishable, confirming the accuracy and reproducibility of our approach.

Intensity normalisation

One significant contribution of our study is a comparison between the IIR and NI metrics for the qualitative assessment of independently acquired MR images.

By its definition, IIR accounts for underlying shifts in the intensity spectrum, while NI includes the standard deviation of the blood pool to account for inter- and intra-patient differences and accordingly for differences in the dynamic range of the images. Consequently, NI led to a more robust statistical model for elucidating the relationship between CV and intensity, compared with IIR, as well as improved reproducibility of the patient-specific association. In particular, the 95% confidence intervals on the intercept and slope estimates for IIR, shown in Figure 5B, were generally larger than the corresponding confidence intervals for NI in Figure 5A. Reproducibility of patient-specific slopes was observed for NI, but not for IIR.

Conduction velocity restitution

No statistically significant effects due to CL were observed, indicating no identifiable CV restitution.

Limitations

In order to obtain high fidelity electrograms, electroanatomical data were limited to the posterior LA, which was anatomically consistent, conducive to placement of the AFocusII mapping catheter tangential to the endocardial surface, and contained a predilection of fibrosis. Sampling

from the posterior wall may have potentially introduced sampling bias. Future studies should incorporate contact sensing catheters to increase robustness of the data collection protocol. This study investigated a persistent AF cohort which has been shown to have more extensive structural and electrical remodelling compared to paroxysmal AF patients. Future studies should include a more heterogeneous group of patients.

The image MR images used in this study were manually segmented to delineate the epicardial wall of the left atrium. As such, errors may have been introduced during the segmentation process.

IIR is defined as the ratio of the wall intensity of the sector to the blood pool mean [19]. However, in this study, IIR was evaluated point-wise as the ratio of the epicardial wall intensity and the mean blood intensity.

Conclusions

Higher LA intensities correspond to lower local myocardial conduction velocities. The scale of measurement of CV and LA wall intensity is crucial in accurately quantifying this relationship, which is found to be of a higher magnitude than previously reported [1]. Importantly, NI, but not IIR, accounts for changes in the dynamic range of LGE-CMRI and improves the quantitative reproducibility of the relationship. Evaluation of the LA substrate with the use of normalised intensity from LGE-CMRI can be potentially used as a minimally invasive tool to predict atrial myocardial conduction properties.

[1] Present address: Johns Hopkins University, 3400 N Charles Street, Baltimore, MD, USA

[2] Present address: 4th Floor, North Wing, St. Thomas' London, UK

References:

1. Fukumoto K, Habibi M, Ipek EG, Zahid S, Khurram IM, Zimmerman SL, Zipunnikov V, Spragg D, Ashikaga H, Trayanova N, et al. Association of Left Atrial Local Conduction Velocity With Late Gadolinium Enhancement on Cardiac Magnetic Resonance in Patients With Atrial Fibrillation. *Circulation: Arrhythmia and Electrophysiology*. 2016;9.
2. Badger TJ, Oakes RS, Daccarett M, Burgon NS, Akoum N, Fish EN, Blauer JJ, Rao SN, Adjei-Poku Y, Kholmovski EG, et al. Temporal left atrial lesion formation after ablation of atrial fibrillation. *Heart Rhythm*. 2009;6:161-8.
3. Tanaka K, Zlochiver S, Vikstrom KL, Yamazaki M, Moreno J, Klos M, Zaitsev AV, Vaidyanathan R, Auerbach DS, Landas S, et al. Spatial distribution of fibrosis governs fibrillation wave dynamics in the posterior left atrium during heart failure. *Circ Res*. 2007;101:839-47.
4. Spach MS and Kootsey JM. The nature of electrical propagation in cardiac muscle. *The American journal of physiology*. 1983;244:H3-H22.
5. Schmidt A, Azevedo CF, Cheng A, Gupta SN, Bluemke DA, Foo TK, Gerstenblith G, Weiss RG, Marban E, Tomaselli GF, et al. Infarct tissue heterogeneity by magnetic resonance imaging identifies enhanced cardiac arrhythmia susceptibility in patients with left ventricular dysfunction. *Circulation*. 2007;115:2006-14.
6. Pontecorboli G, Figueras IVRM, Carlosena A, Benito E, Prat-Gonzales S, Padeletti L and Mont L. Use of delayed-enhancement magnetic resonance imaging for fibrosis detection in the atria: a review. *Europace*. 2017;19:180-189.
7. Habibi M, Lima JA, Khurram IM, Zimmerman SL, Zipunnikov V, Fukumoto K, Spragg D, Ashikaga H, Rickard J, Marine JE, et al. Association of left atrial function and left atrial enhancement in patients with atrial fibrillation: cardiac magnetic resonance study. *Circ Cardiovasc Imaging*. 2015;8:e002 769.
8. McGann C, Kholmovski E, Blauer J, Vijayakumar S, Haslam T, Cates J, DiBella E, Burgon N, Wilson B, Alexander A, et al. Dark regions of no-reflow on late gadolinium enhancement magnetic resonance imaging result in scar formation after atrial fibrillation ablation. *J Am Coll Cardiol*. 2011;58:177-85.
9. Cochet H, Mouries A, Nivet H, Sacher F, Derval N, Denis A, Merle M, Relan J, Hocini M, Haissaguerre M, et al. Age, atrial fibrillation, and structural heart disease are the main determinants of left atrial fibrosis detected by delayed-enhanced magnetic resonance imaging in a general cardiology population. *J Cardiovasc Electrophysiol*. 2015;26:484-92.
10. Ali RL, Cantwell CD, Qureshi NA, Roney CH, Lim B, Sherwin SJ, Siggers JH and Peters NS. Automated fiducial point selection for reducing registration error in the co-localisation of left atrium electroanatomic and imaging data. *2015 37th Annual International Conference of the IEEE Engineering in Medicine and Biology Society (EMBC), Milan*. 2015:1989-1992.
11. Schnabel JA, Rueckert D, Quist M, Blackall JM, Castellano-Smith AD, Hartkens T, Graeme PP, Hall WA, Liu H, Truwit CL, et al. A Generic Framework for Non-rigid Registration Based on Non-uniform Multi-level Free-Form Deformations. *Medical Image Computing and Computer-Assisted Intervention -- MICCAI 2001*. 2001:573--581.

12. Rueckert D, Sonoda LI, Hayes C, Hill DL, Leach MO and Hawkes DJ. Nonrigid Registration Using Free-Form Deformations: Application to Breast MR Images. *IEEE Transactions on Medical Imaging* 1999;18:712 - 721.
13. Studholme C, Hill DL and Hawkes DJ. An overlap invariant entropy measure of 3D medical image alignment. *Pattern Recognition*. 1999;32:71-86.
14. Fitzpatrick JM and West JB. The distribution of target registration error in rigid-body point-based registration. *IEEE Trans Med Imaging*. 2001;20:917-927.
15. Roney CH, Cantwell CD, Qureshi NA, Ali RL, Chang ETy, Lim B, Sherwin SJ, Peters NS, Siggers JH and Ng FS. An automated algorithm for determining conduction velocity, wavefront direction and origin of focal cardiac arrhythmias using a multipolar catheter. *Conf Proc IEEE Eng Med Biol Soc*. 2014:1583-1586.
16. Kojodjojo P, Kanagaratnam P, Markides V, Davies DW and Peters NS. Age-related changes in human left and right atrial conduction. *Journal of Cardiovascular Electrophysiology*. 2005;17:120-127.
17. Cantwell CD, Roney CH, Ali RL, Qureshi NA, Lim B and Peters NS. A software platform for the comparative analysis of electroanatomic and imaging data including conduction velocity mapping. *Conf Proc IEEE Eng Med Biol Soc*. 2014:1591-1594.
18. Kolipaka A, Chatzimavroudis GP, White RD, O'Donnell TP and Setser RM. Segmentation of non-viable myocardium in delayed enhancement magnetic resonance images. *Int J Cardiovasc Imaging*. 2005;21:303-11.
19. Khurram IM, Beinart R, Zipunnikov V, Dewire J, Yarmohammadi H, Sasaki T, Spragg DD, Marine JE, Berger RD, Halperin HR, et al. Magnetic resonance image intensity ratio, a normalized measure to enable interpatient comparability of left atrial fibrosis. *Heart Rhythm*. 2014;11:85-92.
20. Ali RL, Cantwell CD, Roney CH, Qureshi NA, Lim B, Siggers JH, Sherwin SJ and Peters NS. A novel method for quantifying localised correlation of late-gadolinium intensity with conduction velocity. *Computing in Cardiology*. 2014:193-196.
21. Ramanathan C, Ping J, Ghanem R, Ryu K and Rudy Y. Activation and repolarization of the normal human heart under complete physiological conditions. *Proc Natl Acad Sci*. 2006;103:6309-6315.
22. Cantwell CD, Roney CH, Ng FS, Siggers JH, Sherwin SJ and Peters NS. Techniques for automated local activation time annotation and conduction velocity estimation in cardiac mapping. *Comput Biol Med*. 2015;65:229-42.
23. Maleckar MM, Greenstein JL, Giles WR and Trayanova NA. K+ current changes account for the rate dependence of the action potential in the human atrial myocyte. *Am J Physiol Heart Circ Physiol*. 2009;297:H1398-410.
24. Rook MB, van Ginneken AC, de Jonge B, el Aoumari A, Gros D and Jongsma HJ. Differences in gap junction channels between cardiac myocytes, fibroblasts , and heterolo-gous pairs. *The American journal of physiology*. 1992;263:C959-C977.
25. King JH, Huang CL and Fraser JA. Determinants of myocardial conduction velocity: implications for arrhythmogenesis. *Front Physiol*. 2013;4:154.
26. Frustaci A, Chimenti C, Bellocci F, Morgante E, Russo MA and Maseri A. Histological substrate of atrial biopsies in patients with lone atrial fibrillation. *Circulation*. 2007;96:1180-1184.
27. Ciaccio EJ, Chow AW, Kaba RA, Davies DW, Segal OR and Peters NS. Detection of the diastolic pathway, circuit morphology, and inducibility of human postinfarction ventricular tachycardia from mapping in sinus rhythm. *Heart Rhythm*. 2008;5:981-91.

500
501

Patient Characteristics (n=8)	
Age (y)	62±11
Male	5 (62.5)
Mean LA size on TTE (mm)	41±6
MeanCHADS2 score	2.4 (0-5)
Mean left ventricular EF (%)	62±8
Hypertension	3 (37.5)
Diabetes Mellitus	1 (12.5)
Cerebrovascular disease	1 (12.5)
Coronary artery disease	2 (25)
History of heart failure	0 (0)
Duration of persistent AF (months)	19±10.7
Anti-arrhythmic drug therapy (beta-blocker, flecainide and amiodarone)	6 (75)

502

503 Table 1: Clinical demographics of patients.

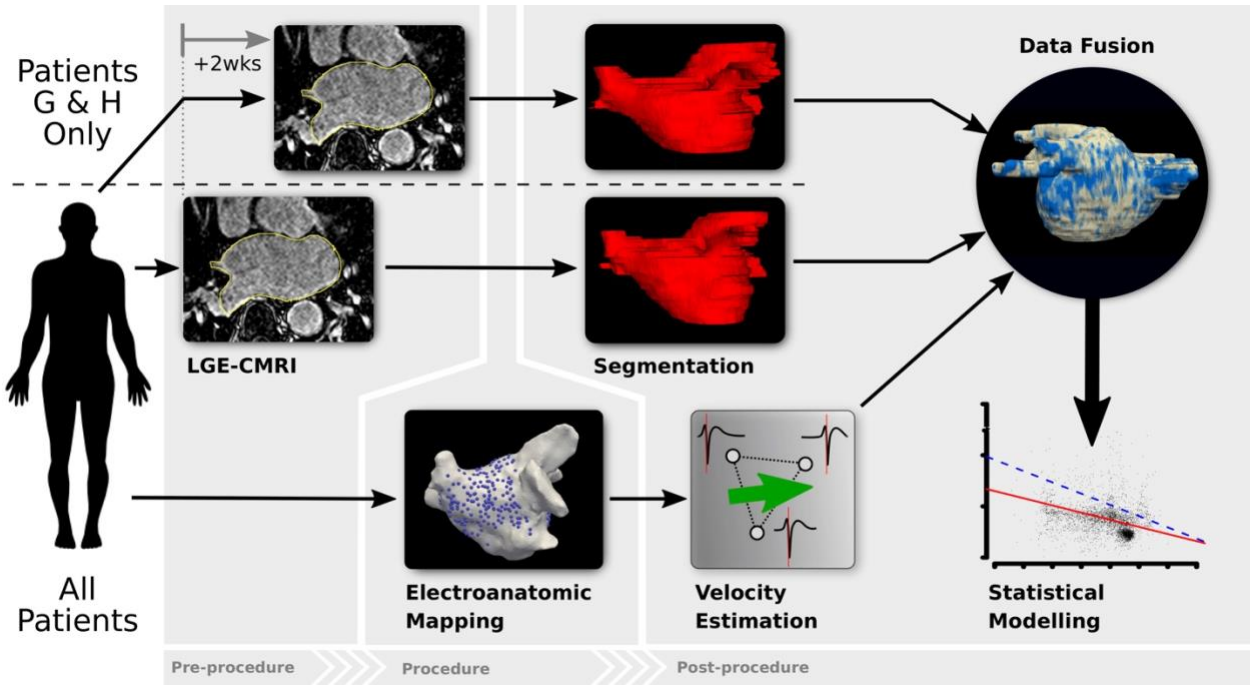

Figure 1*: Diagram of the analysis methodology. All patients undergo LGE-CMRI prior to the ablation procedure (patients G and H had 2 pre-procedural LGE-CMRI to assess reproducibility of LA fibrosis-mapping). Prior to any ablation, LA EAM during pacing is performed. Localised CV is estimated from EAM data and LGE-CMRI images are segmented to estimate fibrosis density. Data is co-registered and fused, after which statistical modelling is undertaken.*

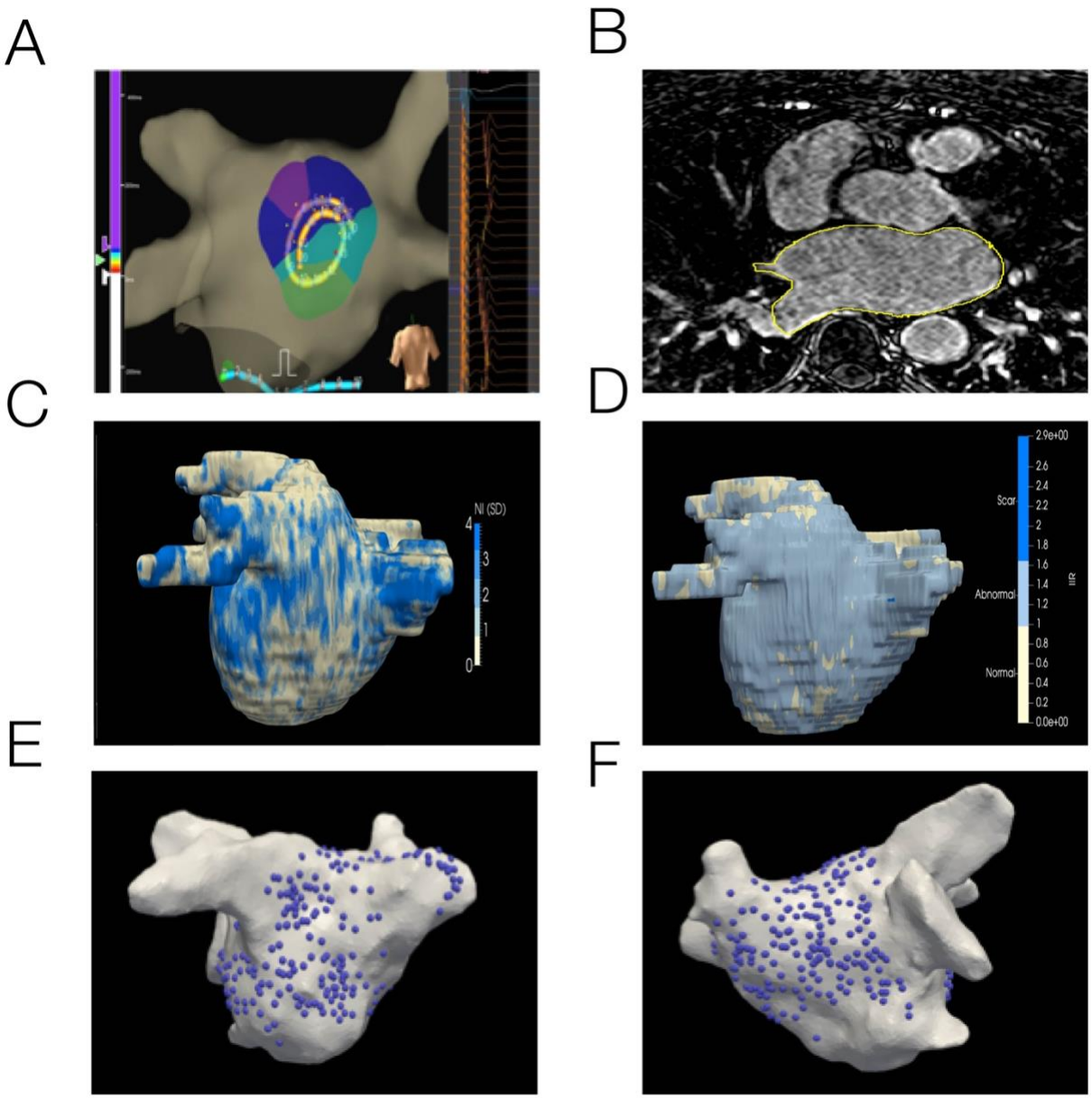

Figure 2: ***A:*** *Ensite™ Velocity mapping system used for collecting endocardial electrograms. The LA was paced over a range of CLs and the acquired unipolar electrograms are shown in the right panel.* ***B:*** *LGE-CMRI axial slice with manual segmentation delineated in yellow* ***C:*** *Illustrative patient-specific map NI.* ***D:*** *Illustrative patient-specific map of IIR for same patient as C.* ***E*** *and* ***F****: Distribution of electrograms on the posterior and anterior walls of the LA respectively.*

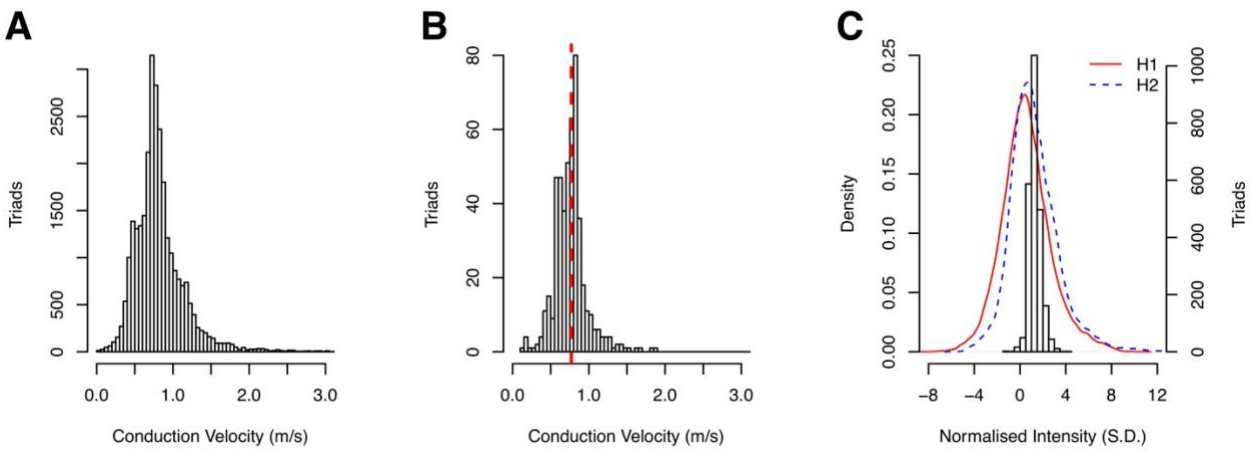

*Figure 3: **A:** Distribution of CV measurements in the study. **B:** Comparison of local CV measurement distribution with regional CV estimate (red dashed line). **C:** Distribution of sampled NI for patient H second scan and the density of NI across entire atrial surface for both*

scans.

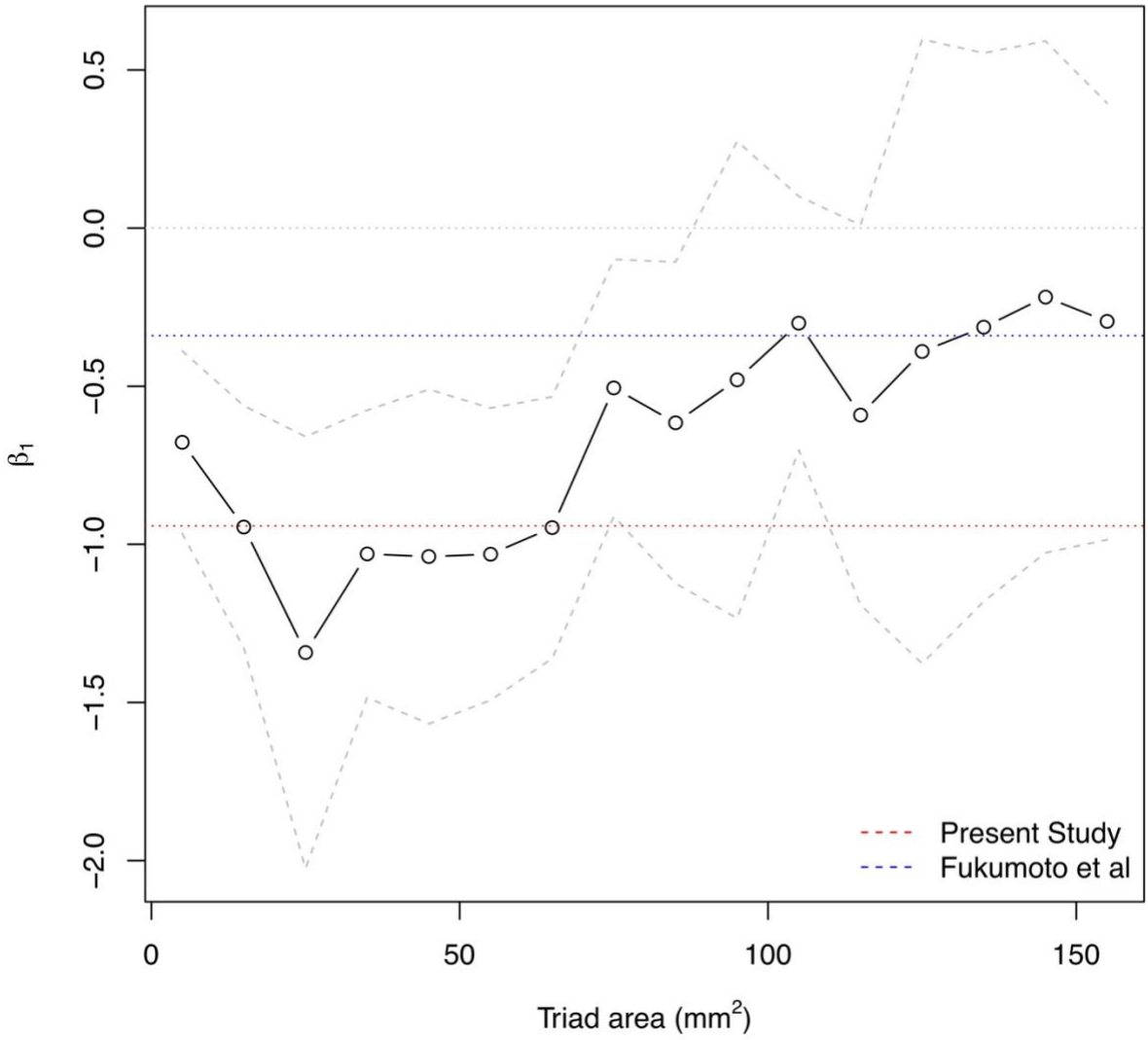

Figure 4: Influence of measurement area on the overall β_1 estimate for association of CV with NI. Solid area denotes 95% confidence intervals. Larger measurement areas lead to lower magnitude β_1 estimate. The dotted red line indicates final β_1 estimate from present model for localised measurements with areas < 80mm^2. The dotted blue line indicates beta estimate from Fukumoto et al[1].

530

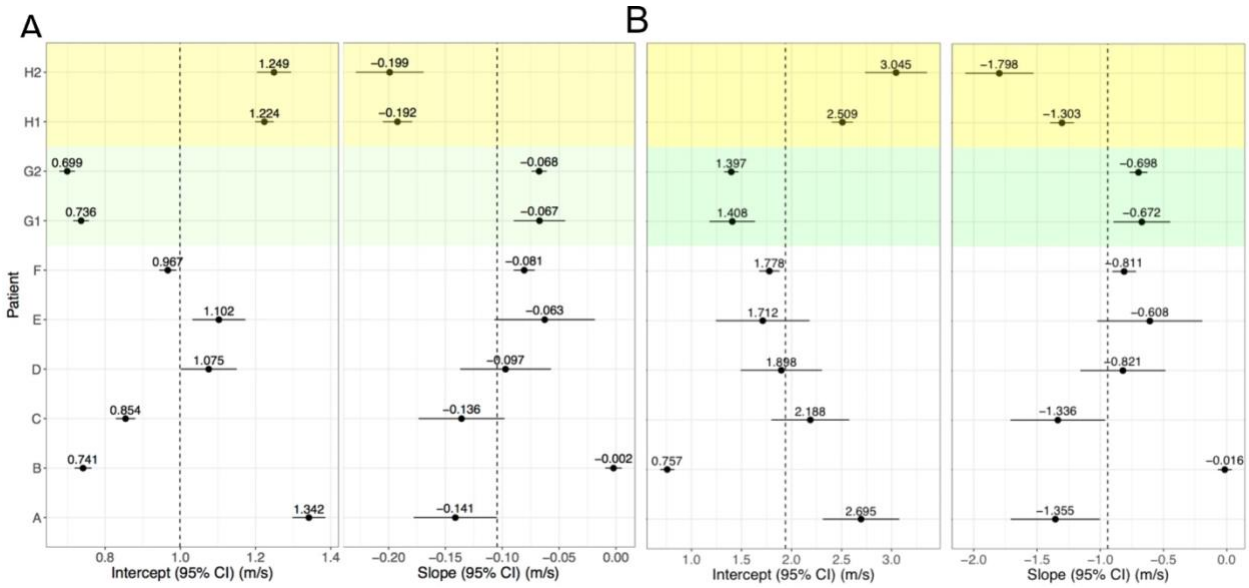

531

532 *Figure* 5*: Per-patient model intercepts (left) and slopes (right) for NI (A) and IIR (B). Values*

533 *indicate the per-patient difference from the model's overall intercept () and slope (NI: 1.00 m/s,*

534 *= -0.104; IIR: =1.94 m/s, = -0.942. G1, G2 and H1, H2 correspond to repeat analyses of patients*

535 *G and H for assessing reproducibility.*

536
537